Mechanism of the polarization control in intracavity-contacted VCSEL with rhomboidal oxide current aperture

M A Bobrov[1], N A Maleev[1], S A Blokhin[1], A G Kuzmenkov[2,1], A P Vasil'ev[2,1], A A Blokhin[1], M M Kulagina[1], Yu A Guseva[1], S I Troshkov[1], V M Ustinov[1,2,3]

[1] Ioffe Institute, Politekhnicheskaya 26, St. Petersburg, 194021 Russia
[2]Submicron Heterostructures for Microelectronics Research and Engineering Center of the RAS, St Petersburg, Russia
[3]Peter the Great St. Petersburg Polytechnic University, St Petersburg, Russia
E-mail: *Bobrov.mikh@gmail.com*

Abstract. The possible mechanisms of the polarization control in single-mode intracavity-contacted vertical-cavity surface-emitting lasers (IC-VCSELs) with the rhomboidal selectively-oxidized current aperture were investigated. It was found that the lasing emission polarization of all single-mode VCSELs is fixed along the minor diagonal of the rhomboidal-shape aperture (the $[\bar{1}10]$ direction). Numerical modelling of carrier transport did not reveal any sufficient injection anisotropy in the laser active region, while the transverse optical confinement factors calculated for the fundamental mode with two orthogonal polarizations are identical. Optical loss anisotropy and/or gain anisotropy are the most likely mechanisms of inducing the polarization fixation.

1. Introduction
A GaAs-based vertical-cavity surface-emitting lasers (VCSELs) are attractive low-cost laser source for high-speed data communication systems, optical interconnects and different sensors [1]. New VCSEL applications (compact atomic clock and magnetometer) require single-mode temperature-stable operation with fixed linear polarization [2]. While the conventional VCSELs with small oxide aperture diameters demonstrate stable fundamental transverse mode operation, the combination of cylindrical symmetry and isotropic gain leads to polarization uncertainty and instability [3]. Despite a number of efforts (polarization-dependent gain, asymmetric resonators, polarization-dependent mirrors, external optical feedback) this issue is still under investigation [4-7].
In this work we discuss possible mechanisms for polarization control in single-mode VCSELs containing rhomboidal selectively-oxidized current aperture and intracavity contacts (IC).

2. VCSEL design
Since it is challenging to achieve both high conductivity and low loss using fully-doped AlGaAs distributed Bragg reflectors (DBRs) grown by molecular beam epitaxy (MBE), VCSEL design with two relatively high-doped contact layers sandwiched between undoped DBRs and optical microcavity was widely used [8]. To improve the conventional short-wavelength IC-VCSEL design we propose to embed a few pairs of doped $Al_{0.15}Ga_{0.85}As/Al_{0.9}Ga_{0.1}As$ DBR (so called composite lattice) between InGaAlAs-based active region and the buried AlGaAs contact layers to decrease the optical field amplitude in high-doped layers, to employ a top dielectric SiO_2/TiO_2 DBR for better optical confinement and to insert p^+-GaAs contact layer directly between the electrical p-contact and the p-

$Al_{0.15}Ga_{0.85}As$ contact layer to decrease contact resistance and free carrier absorption [9]. Selective wet oxidation of thin AlAs/AlGaAs aperture layer embedded into the p-doped composite lattice was used to create lateral confinement for both the injected current and the optical field. Device fabrication steps include mesa etching, selective oxidation, p- and n-contact formation, top dielectric DBR deposited after local window opening in p^+-GaAs contact layer, planarization and contact pads deposition. The details of the VCSEL epitaxial structure and processing can be found in [9]. The schematic cross-section of the processed 850 nm IC-VCSEL is shown in figure 1.

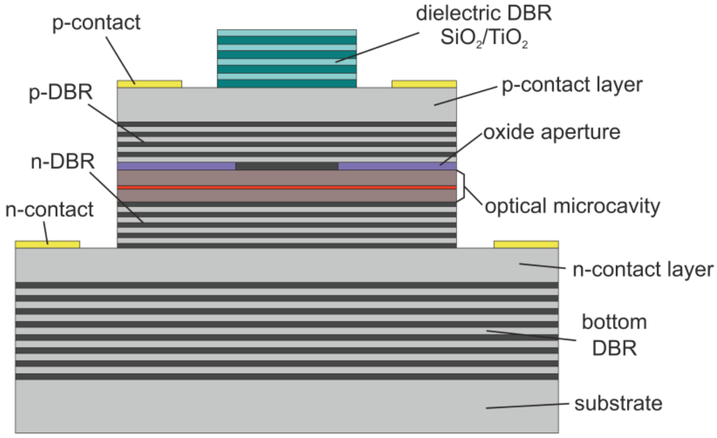

Figure 1. Schematic cross-section of 850 nm oxide-confined VCSEL with dielectric DBR and intra-cavity contacts.

3. Results and discussion

Figure 2 shows the light output power-current characteristics and the typical lasing spectra at 20°C and 80°C for the InGaAlAs IC-VCSELs with aperture size of about 2.5 μm. The devices demonstrate continuous-wave single-mode lasing at 845-852 nm with side-mode suppression ratio (SMSR) higher than 30 dB with output power more than 1.5 mW, threshold current less than 0.9 mA and orthogonal polarization suppression ratio (OPSR) higher than 20 dB for operation temperature of 20-80ºC. No polarization switching was observed through the entire current and temperature range. According to the near field studies (see inset in Figure 2.b), the IC-VCSELs with current aperture size less than 10 μm have a rhomboidal shape of oxide aperture with the major diagonal along the $[110]$ direction, which is caused by crystallographic sensitivity of oxidation speed of AlAs layers [10]. Moreover the emission polarization is always fixed along the minor diagonal of the rhomboidal-shape aperture (along the $[\bar{1}10]$ direction).

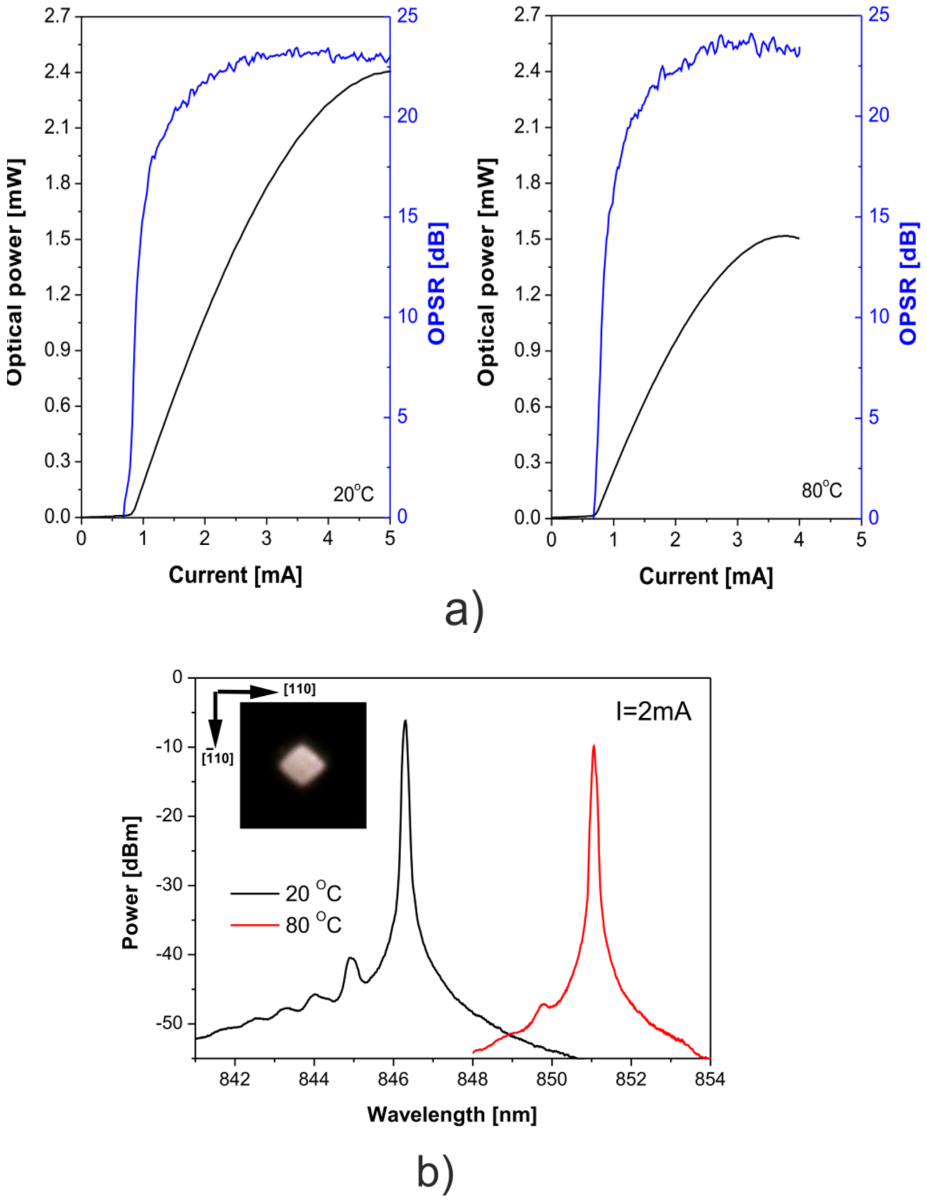

Figure 2. 850 nm IC-VCSEL with aperture size of about 2.5 μm: (a) Output power and OPSR as function of current at different temperatures; (b) Lasing spectra at 2 mA for different temperatures. Inset: near-field image below threshold current.

The observed polarization behavior can be attributed to the electro-optic effect [11], which caused a refractive index ellipsoid with [110] and [$\bar{1}$10] as the principal axes, however this effect is inherently unstable (rotation or switching of the polarization with current or temperature). To clarify the possible mechanism of the strong polarization stability, the simplified numerical modeling of optical mode and carrier distributions were done.

The 2D microcavity optical field was calculated using effective index method [12]. Figure 3.a shows the refractive index and the corresponding electric field intensity profile for the investigated 850 nm IC-VCSEL. For the rhomboidal microcavity the fixation of the longitudinal component of electric field E_z along one of two possible directions (along the major or minor diagonals) was observed (see

Figure 3.b). According to the calculated distribution of the transverse component of electric field E_{xy}, the transverse optical confinement factor for two orthogonal polarizations of the fundamental mode differs less than 3%, which is too small for the stable polarization control.

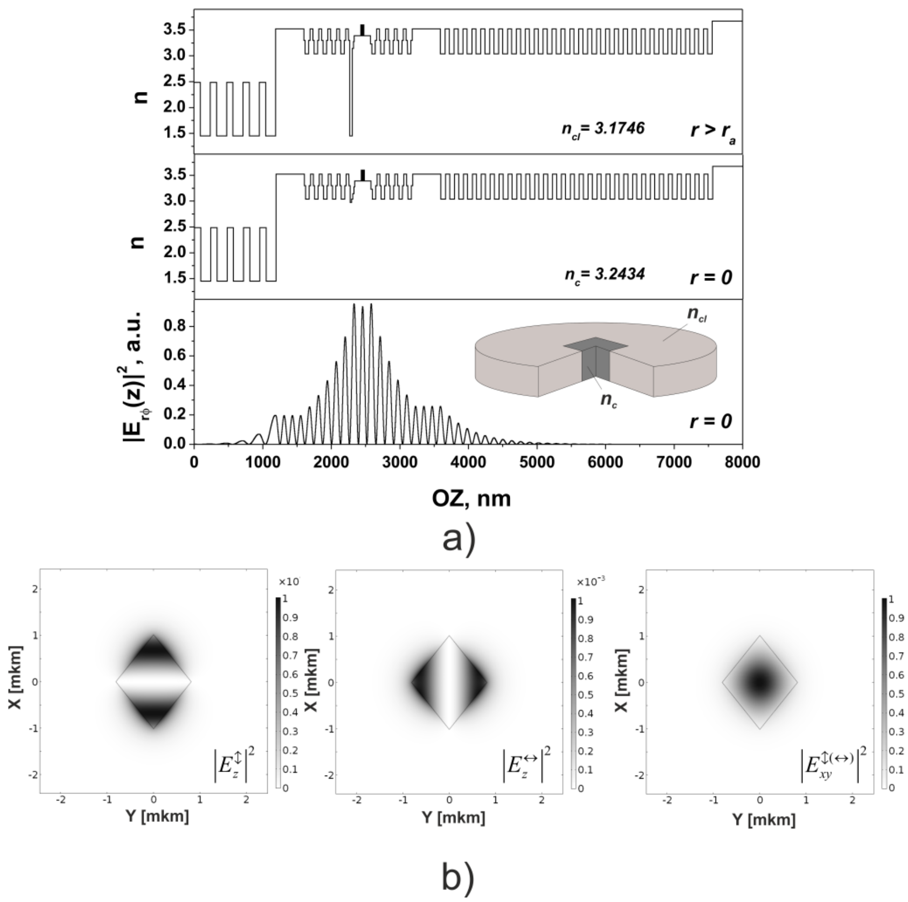

Figure 3. Optical calculation for 850 nm IC-VCSEL: (a) Refractive index profile and normalized electric field intensity versus distance from the top IC-VCSEL surface. Inset: the schematic effective waveguide with the rhomboidal selectively-oxidized current aperture; (b) The fundamental mode distribution of longitudinal (E_z) and transverse (E_{xy}) components of electric field for two possible polarizations.

To perform 3D carrier transport numerical simulation, the composite lattices were replaced by the single layer with the anisotropic carrier mobility (see inset in Fig.4.a). The carrier spatial distributions below lasing threshold for the simplified VCSEL structure revealed the carrier concentration near the rhombus acute angles for multimode devices with aperture size more than 5 µm (see inset in Figure 4.b). Above lasing threshold the anisotropic carrier distribution on the oxide aperture area can be enhanced due to the spatial hole-burning effect. However, the carrier distributions for the aperture size less than 5 µm are more uniform into the aperture and, hence, the observed polarization control cannot be explained by the injection anisotropy in the laser active region.

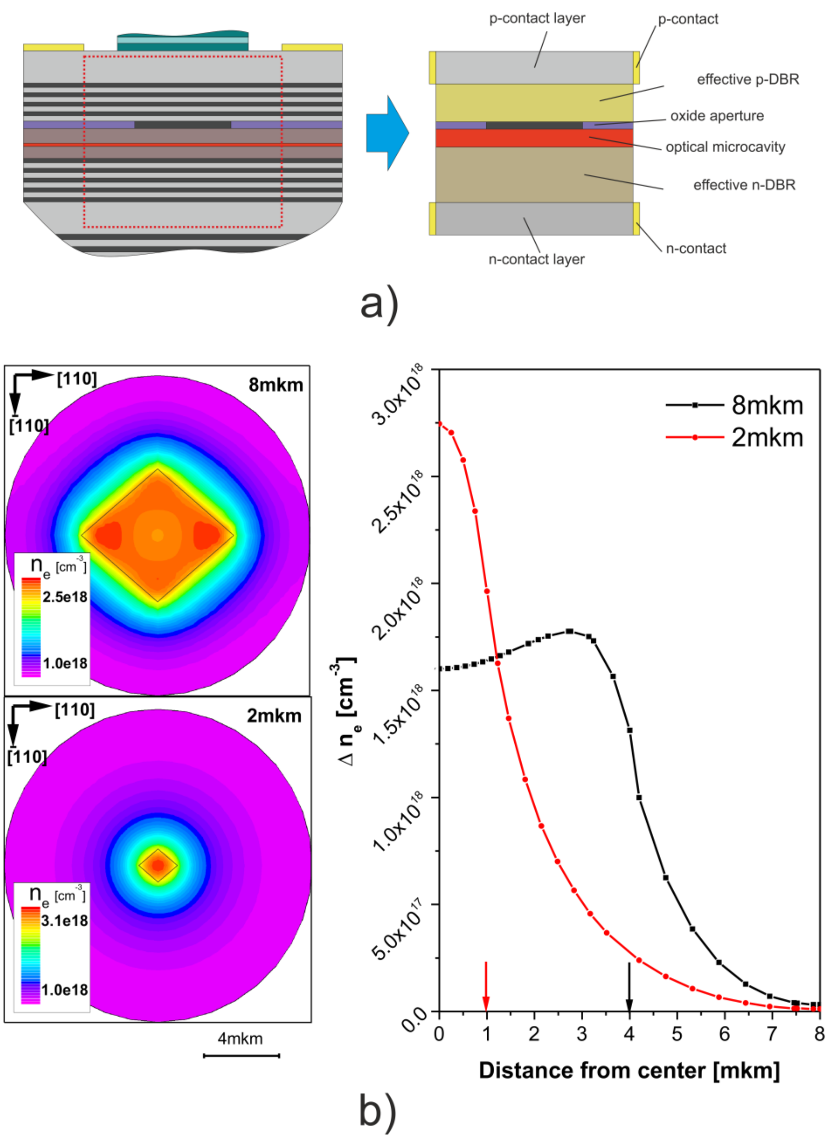

Figure 4. Carrier calculation for 850 nm IC-VCSEL: (a) Scheme of the simplified IC-VCSEL with the rhomboidal-shape current aperture; (b) Carrier distributions and corresponding cross-section profiles for two aperture size about 2 µm and 8 µm.

We attribute the polarization fixation to the polarization-dependent scattering losses inside the asymmetric VCSEL cavity, for example, the light diffraction on the rhomboidal-shape oxide aperture. On the other hand, the spontaneous emission of such IC-VCSELs is partially polarized along the $[\bar{1}10]$ direction, which can be associated with the gain anisotropy of InGaAlAs-based active region. More detailed modelling based on the real design of the optical microcavity and/or the investigation of the spontaneous emission via the oxide aperture shape for IC-VCSELs is necessary to clarify the origin for the polarization fixation along the $[\bar{1}10]$ direction.

4. Conclusion

The alternative approach for single-mode polarization-stable VCSELs based on rhomboidal selectively-oxidized current aperture combined with intracavity contacts was discussed. The single-mode devices have output power more than 1.5 mW and threshold current less than 0.9 mA into the temperature range of 20-80ºC. The lasing emission is polarized along the minor diagonal of the rhomboidal selectively-oxidized current aperture (oriented along the $[\bar{1}10]$ direction). Optical simulation of the effective waveguide with the rhomboidal-shape core results in the similar transverse optical confinement factor for two orthogonal polarizations of the fundamental mode. On the other hand, the carrier transport numerical simulation of single-mode devices did not reveal the significant anisotropic carrier distribution on the oxide aperture area. The anisotropy of optical losses in the rhomboidal microcavity and/or the gain anisotropy in the strained quantum wells seems to be responsible for the observed polarization fixation along the $[\bar{1}10]$ direction.

Acknowledgments
This work was supported in part by the Ministry of Education and Science of the Russian Federation (grant № 14.607.21.0001, unique ID RFMEFI60714X0001).

References
[1] R. Michalzik, VCSELs: Fundamentals, Technology and Applications of Vertical-Cavity Surface-Emitting Lasers, Berlin: Springer-Verlag, 2013.
[2] D.K. Serkland, G.M. Peake, K.M. Geib, R. Lutwak, R.M. Garvey, M. Varghese, M. Mescher, "VCSELs for atomic clocks", *Proc. SPIE* **6132** 613208, 2006.
[3] G. Verschaffelt, K. Panajotov, J. Albert, B. Nagler, M. Peelers, J. Danckaert, I. Veretennicoff and H. Thienpont, "Polarisation switching in vertical-cavity surface-emitting lasers: From experimental observations to applications," *Opto-Electron. Rev.* **9** 257–268, 2001.
[4] N. Nishiyama, M. Arai, S. Shinada, M. Azuchi, T. Miyamato, F. Koyama, K. Iga, "Highly strained GaInAs/GaAs quantum well vertical-cavity surface-emitting laser on GaAs (311)B substrate for stable polarization operation, " *IEEE J. Select. Topics Quantum Electron*. **7** 242, 2001.
[5] Y. Sato, K. Furuta, T. Katayama, H. Kawaguchi, "Polarization switching in vertical-cavity surface-emitting lasers by asymmetrical current injection," *IEEE Photon. Technol. Lett.* 20, 1446, 2008.
[6] S. Riyopoulos and E. Nhan, "Polarization selection due to scattering losses in nonaxisymmetric vertical cavity surface emitting laser cavities," *Appl. Phys. Lett.* **85** 3038, 2004.
[7] J.M. Ostermann, P. Debernardi, R. Michalzik, "Optimized integrated surface grating design for polarization-stable VCSELs," *IEEE J. Quantum Electron*. **42** 690, 2006.
[8] D.L. Huffaker, D.G. Deppe, "Intracavity contacts for low-threshold oxide-confined vertical-cavity surface-emitting lasers," *IEEE Photon. Technol. Lett*. **11** 934–936, 1999.
[9] N.A. Maleev, A.G. Kuz'menkov, M.M. Kulagina, Yu.M. Zadiranov, A.P. Vasil'ev, S.A. Blokhin, A.S. Shulenkov, S.I. Troshkov, A.G. Gladyshev, A.M. Nadtochiy, M.M. Pavlov, M.A. Bobrov, D.E. Nazaruk, V.M. Ustinov, "Single-spatial-mode semiconductor VCSELs with a nonplanar upper dielectric DBR," *Semiconductors* **47** 993, 2013.
[10] K.D. Choquette, K.M. Geib, C.I.H. Ashby, R.D. Twesten, O. Blum, H.Q. Hou, D.M. Follstaedt, B.E. Hammons, D. Mathes, R. Hull, "Advances in selective wet oxidation of AlGaAs alloys," *IEEE J. Select. Topics Quantum Electron.* **3** 916, 1997.
[11] M.P. Van Exter, A.K. Jansen van Doorn and J.P. Woerdman, "Electrooptic effect and birefringence in semiconductor vertical-cavity lasers," *Phys. Rev. A, Gen. Phys.* **56** 845, 1999.
[12] G.R. Hadley, "Effective index model for vertical-cavity surface-emitting lasers", *Opt. Lett.* **20** 1483, 1995.